

## X-Band Dielectric and Microwave-Absorbing Properties of the Incompletely Carbonized Polyacrylonitrile Cloth

Zhibin Huang, Wenbo Kang, Xiufeng Tang, Yuchang Qing, Fa Luo

State Key Laboratory of Solidification Processing, Northwestern Polytechnical University, Xi'an 710072, China

Correspondence to: Z. Huang (E-mail: huangzhibin83@163.com)

**ABSTRACT:** Incompletely carbonized polyacrylonitrile (PAN) cloths were prepared by heating stabilized PAN cloth at 600–800°C in different atmosphere. Their X-band dielectric and microwave-absorbing properties were investigated. Results showed that the complex permittivity constantly increased with the increasing heating temperature due to the growth of carbon sheets. Conversely, the cloths carbonized in air exhibit lower complex permittivity than those carbonized in nitrogen because the reaction with oxygen restricts the progress of carbonization. The reflection loss below  $-10$  dB can be obtained in X band for the sample carbonized at 650°C for 2 h in air. © 2012 Wiley Periodicals, Inc. *J. Appl. Polym. Sci.* 129: 1068–1073, 2013

**KEYWORDS:** dielectric properties; crystallization; fibers

Received 6 August 2012; accepted 29 October 2012; published online 23 November 2012

DOI: 10.1002/app.38773

### INTRODUCTION

In recent years, microwave absorbing and shielding materials continue attracting considerable interests in both commercial and military fields. Carbon materials, such as carbon nanotubes,<sup>1</sup> carbon black,<sup>2</sup> graphite,<sup>3</sup> and carbon fibers (CFs),<sup>4</sup> have been widely used to fabricate microwave absorbing and shielding materials with different insulating matrix.<sup>5</sup> The approaches used for manufacturing microwave absorbing and shielding materials are different according to the matrix. For the commonly used polymer matrix, its composites with carbon absorber can be simply fabricated by blending and curing processing under 200°C. While ceramic matrix, which is usually adopted to fabricate structural microwave-absorbing materials, has to sinter at much higher temperature than polymer matrix. To prevent the decomposition of carbon absorber, the sintering processing usually carried out in the protection of inert atmosphere.

In the aforementioned carbon materials, CF is one of the most used carbon materials in microwave absorbing and shielding applications.<sup>6,7</sup> Many researchers report the dielectric and microwave-absorbing properties of completely carbonized commercial CF.<sup>4–7</sup> However, comparing with the completely carbonized CF, incompletely carbonized CF may be more suitable for fabricating microwave-absorbing materials due to the adjustable permittivity.

Currently, 90% of commercial CFs are produced from polyacrylonitrile (PAN) precursors.<sup>8</sup> During carbonization procedure,

PAN polymers are gradually converted to carbon structure, causing the decrease of room temperature resistivity from  $10^7$ – $10^8$   $\Omega\cdot\text{cm}$  to  $10^{-3}$   $\Omega\cdot\text{cm}$ .<sup>9</sup> The dielectric properties also change synchronously with the progress of carbonization. Xie et al.<sup>10</sup> prepared a series of incompletely carbonized PAN hollow fibers cured at temperature ranging from 550 to 950°C in nitrogen atmosphere. They found carbonization temperature (550–950°C) has significant influence on the microwave-absorbing properties of hollow CFs.

In this article, the influences of carbonization atmosphere on the dielectric properties were mainly investigated. We expected to regulate the dielectric properties of PAN fibers for microwave-absorbing application by means of changing carbonization temperature and atmosphere. A series of incompletely carbonized PAN cloths (ICPCs) were prepared by carbonizing PAN cloths at temperatures ranging from 600 to 800°C in low-pressure air or nitrogen atmosphere. The structure, dielectric, and microwave-absorbing properties of ICPC were examined.

### EXPERIMENTAL

#### Stabilized PAN Cloth

The Stabilized PAN cloth (SPC, Jiyan Carbon, Jilin, China) as starting stuff was two-dimensional orthogonal braided with mutually perpendicular tows (as shown in Figure 1), in which a single tow contains 6000 monofilaments of 10  $\mu\text{m}$  diameter. Before carbonization, the SPC was ultrasonically rinsed in distilled water and then cut into the size of 80  $\times$  40  $\times$  0.4 mm<sup>3</sup>.

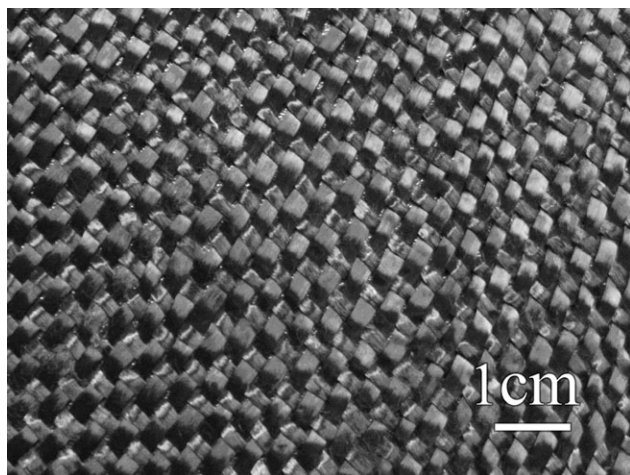


Figure 1. Optical micrograph of SPC.

### Carbonization Process

Before carbonization, the furnace was introduced in different gases (air or nitrogen), then pumped by vacuum pumping system. The above steps were repeated for three times, and the pressure in the chamber is finally maintained at 0.2 Pa throughout the process of carbonization. The SPC (with the size of  $80 \times 40 \times 0.4 \text{ mm}^3$ ) was carbonized in a conventional vacuum sintering furnace with strictly controlled heating rate of  $10^\circ\text{C}/\text{min}$  from room temperature to different heating temperatures ( $600\text{--}800^\circ\text{C}$ ), and then maintained at that level for 2 h. After carbonization, the samples were furnace-cooled to room temperature in 1 atm nitrogen.

### Dielectric Measurement

The complex permittivity  $\epsilon(f)$  of the coatings was measured by wave-guide method in X-band using a network analyzer (E8362B, Agilent technologies, Palo Alto, CA). The multilayer testing specimens have sheet shape of  $22.86 \times 10.16 \text{ mm}^2$  and about 2 mm in thickness.

### Electric Conductivity

The electric conductivity was calculated by dividing the length of fiber yarn (10 mm) by the resistance and the cross-sectional area of the fiber yarn. Two equations as below are applied to calculate the electric conductivity.

$$R = SL/A = SL(\pi D^2/4) \quad (1)$$

$$K = 1/\sigma \quad (2)$$

where R: resistance ( $\Omega$ ), L: length (m), A: cross-sectional area ( $\text{m}^2$ ), D: diameter (m), S: specific resistance ( $\Omega \text{ m}$ ),  $\sigma$  conductivity ( $\Omega^{-1} \text{ m}^{-1}$ ).

### Characterization

The TESCAN VEGA-II scanning electron microscopy (SEM) was used to characterize the microstructures. An X-ray diffractometer (XRD, Philips X'Pert diffractometer) with  $\text{Cu K}\alpha$  radiation was used to determine the structure of cloths. In addition to the XRD, Raman spectroscopy was also used to investigate the structural changes. Raman spectra were obtained on a

Renishaw in via system equipped with a Spectra Physics Ar<sup>+</sup> Laser (514.5 nm, 5 mW).

## RESULTS AND DISCUSSION

### Characterization

X-ray diffraction was carried out to examine the structure variation of SPC during carbonization. As shown in Figure 2, ICPCs exhibit only a broad peak at about  $2\theta = 26^\circ$ , corresponding to the (0 0 2) diffraction of graphite structure, whereas this peak is unobvious for SPC, which can be attributed to the formation of conducting carbon sheet structures in the SPC during carbonization. It also can be observed that the (0 0 2) peaks of the samples carbonized in air are obviously broader than those in nitrogen, indicating the grain size (layer plans) of carbon sheets is smaller in case of carbonization in air. In addition, the absence of (1 1 0) peak of graphite structure indicates that the ICPCs in this work are nongraphitized carbon sheet and far from completely graphitized structure.

It is also noteworthy that there is a weak reflection peak at  $2\theta$  range  $15\text{--}20^\circ$  for the samples carbonized in air. This peak is associated with remnant linear segments and disoriented molecular chains, which should have been removed during the carbonization processing normally.<sup>11</sup> We believe the appearance of this peak can be attributed to the attack of oxygen. As shown in Figure 3, the fiber carbonized in air shows visible roughness and deep pits on the whole fiber surface, whereas the fiber carbonized in nitrogen is smooth without deep pits. It suggests that oxygen in air attacks and removes the surface structures of the fiber, forming visible pits on the surface. The inner surface of the fiber, which was composed of disordered structures, is exposed, leading to the appearance of the broad peak at  $2\theta$  range  $15\text{--}20^\circ$ .<sup>12</sup>

In addition to the XRD, Raman spectroscopy is also used to investigate the structural changes. Figure 4 shows the Raman spectra of ICPC in the region from  $1000$  to  $1800 \text{ cm}^{-1}$ . All curves exhibit two relatively broad Raman bands, one around  $1340 \text{ cm}^{-1}$  called D peak (disordered or amorphous), and

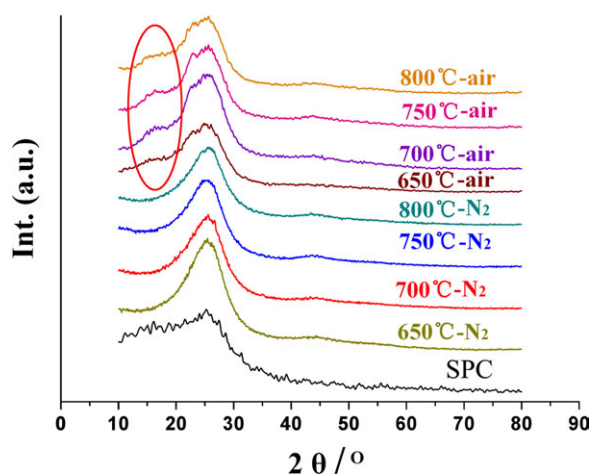
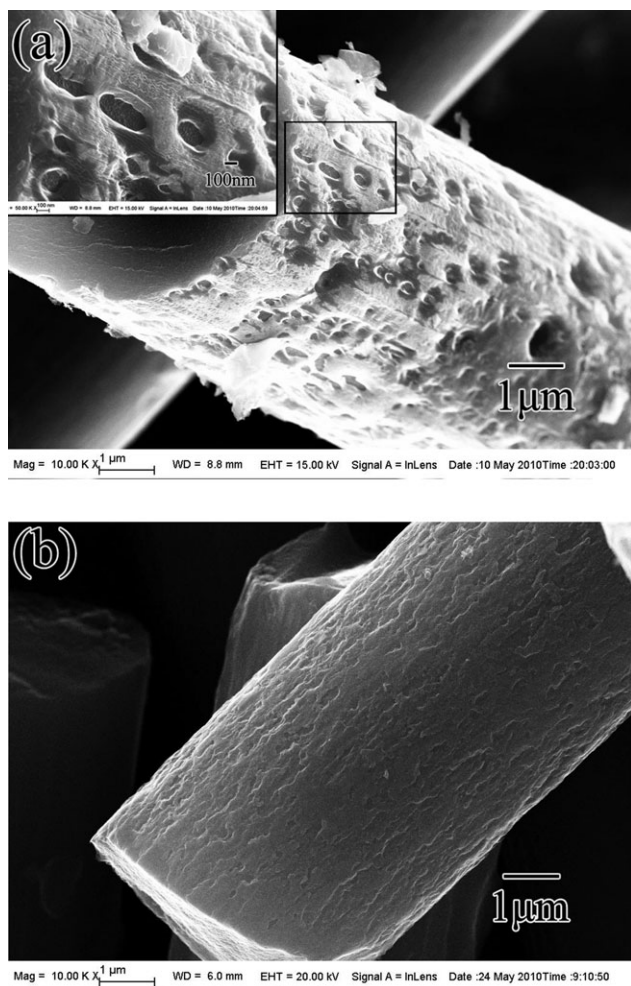


Figure 2. XRD patterns of ICPC and SPC. [Color figure can be viewed in the online issue, which is available at [wileyonlinelibrary.com](http://wileyonlinelibrary.com).]



**Figure 3.** SEM images of ICPC carbonized at 700°C for 2 h (a) in air and (b) in nitrogen. The inset in (a) is the closeup view.

another around  $1590\text{ cm}^{-1}$  called G peak (graphite). The D peak is invisible in perfect graphite and only becomes active in the presence of disorder. Therefore, combined with the analysis of XRD and Raman, it is clearly confirmed that the ICPCs in this work are far from graphitized structure.

The band area ratio  $I_D/I_G$  of Raman spectra, which is known as an important parameter characterizing the extent of carbonization,<sup>13</sup> is listed in Table I. As can be seen,  $I_D/I_G$  value increases with the rising heating temperature, which is contrary to the commonly used TK equation<sup>14</sup> because higher carbonization temperature always causes larger graphite crystalline size.<sup>8,15</sup>

$$\frac{I_D}{I_G} = \frac{C(\lambda_L)}{L_a} \quad (3)$$

where  $L_a$  is the in-plane size of the basic carbon sheets,  $C(\lambda_L)$  is a wavelength-dependent prefactor. The reasonable explanation of this phenomenon is that the TK equation [eq. (3)] is not applicable here when the crystalline size is very small.<sup>16</sup> For crystallite sizes  $L_a$  below 2 nm, Ferrari and Robertson proposed the following correlation<sup>17</sup>:

$$\frac{I_D}{I_G} = C'(\lambda_L)L_a^2 \quad (4)$$

where  $C'(\lambda_L)$  represents a wavelength-dependent prefactor. According to this equation, the larger  $I_D/I_G$  value represents larger  $L_a$  of carbon sheets, which coincides with the observation in Table I. As the structure of ICPC in this work is far from graphite structure, it is expected that the carbon sheets are very small when the carbonization temperature is far lower than it reported in many other literature.<sup>8,16,18,19</sup>

In addition, the carbonization atmosphere also has obvious influences on the  $I_D/I_G$  values. The fibers carbonized in air exhibit lower  $I_D/I_G$  values than those in nitrogen. This also can be attributed to the influence of oxygen, which restricts the growth of carbon crystallites in ICPC.

### Complex Permittivity

Figure 5 exhibits the complex permittivity of the ICPC carbonized at 600 to 800°C in nitrogen. A visible increase of both the real part ( $\epsilon'$ ) and imaginary part ( $\epsilon''$ ) of the permittivity with the increase of heating temperature is observed in all the samples. In addition, the complex permittivity tends to decrease with increasing frequency and show frequency dependence in the whole frequency range.

$\epsilon'$  is known as the expression of polarization ability of materials. In this case, the increasing of  $\epsilon'$  may be mainly attributed to electronic relaxation polarization associated with the growth of carbon sheets. As we know, SPC is an insulating material with low  $\epsilon'$  and approximately zero dielectric loss. During carbonization, its dielectric properties extremely change with the formation of carbon sheets. As illustrated in Figure 6, the carbon sheets are equivalent to conductive filler embedded in the insulating polymer and amorphous carbon. That is, the whole ICPC materials can be viewed as conductor/dielectric composite somehow. Each carbon sheet is an electrical dipole, in which the confined free electrons and/or weakly bound electron in individual carbon sheet respond rapidly to alternating electromagnetic field. So, the moveable electrons vibrate in carbon sheets when subjected to alternating electrical field, which contribute

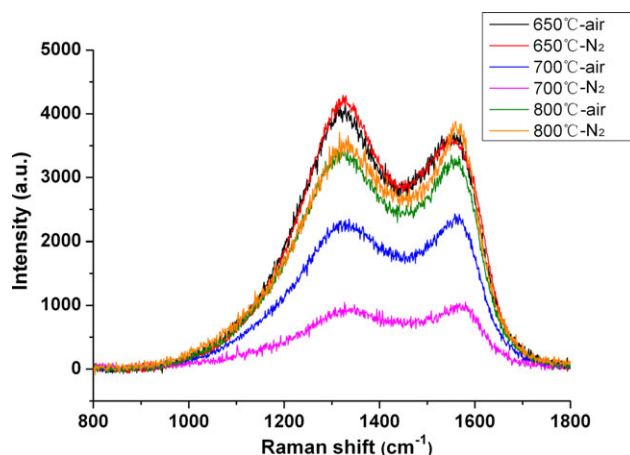


**Figure 4.** Raman spectra of ICPC. [Color figure can be viewed in the online issue, which is available at [wileyonlinelibrary.com](http://wileyonlinelibrary.com).]

**Table I.**  $I_D/I_G$  Values of the ICPC Calculated from Raman Results

Sample code	650°C-air	700°C-air	800°C-air	650°C-N <sub>2</sub>	700°C-N <sub>2</sub>	800°C-N <sub>2</sub>
$I_D/I_G$	3.794	3.807	4.131	3.843	3.975	5.191

to the increase of  $\epsilon'$ . Obviously, the electronic relaxation polarization ability is improved as more carbon sheets form in ICPC.

Conversely, the  $\epsilon''$ , which represents capacity of dielectric loss in the microwave frequency, also increases with the increasing carbonization temperature. In this case, polarization losses ( $\epsilon_1''$ ) and electric conductance loss ( $\epsilon_C''$ ) are dominant types of dielectric losses.<sup>20</sup>

As we know, carbon sheets conduct electricity in carbocycle plane because of the formation of  $\mu$ -cloud. As illustrated in Figure 6(c), the free electrons migrate within individual carbon sheet (corresponding to polarization losses) or hopping among the carbon sheets (corresponding to conductance loss) when subjected to alternating electrical field. To overcome the electrical resistance, the microwave energy simultaneously converts to thermal energy.

It is obvious that the  $\epsilon_C''$  and  $\epsilon_1''$  of ICPC are mainly related to the hopping electrons resistance among carbon sheets and the migrating electrons resistance within carbon sheets, respectively. According to the free electric theory and approximately considering the two resistances as an equivalent series circuit, we can get the following equation<sup>21</sup>:

$$\epsilon''_C + \epsilon''_1 = \sigma / (\omega \cdot \epsilon_0) \propto \left( \frac{1}{R_{\text{hop}} + R_{\text{mig}}} \right) / (\omega \cdot \epsilon_0) \quad (5)$$

where  $\sigma$  is a.c. conductivity of ICPC.  $R_{\text{hop}}$  and  $R_{\text{mig}}$  are the electrical resistivity of electron hopping and electron migration, respectively.  $\omega$  is the angular frequency. Apparently, the increase of carbon sheets in both size and number will decrease the  $R_{\text{hop}}$ , owing to the constantly shortened distance among the carbon sheets. As a result, the free electrons are more and more prone to hop among the carbon sheets with consequent increase of  $\epsilon_C''$ , which is confirmed by the electric conductivity results shown in Table II.

Figure 7 exhibits the complex permittivity of the samples carbonized at 600 to 800°C in air. Comparing Figure 5 with Figure 7, both  $\epsilon'$  and  $\epsilon''$  are lower in case of carbonization in air than

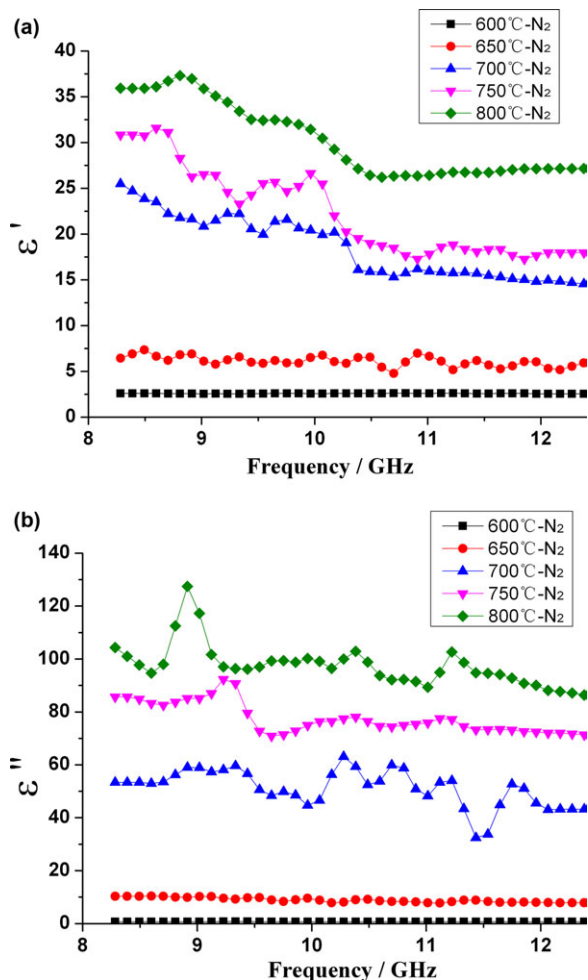


**Figure 5.** (a) The  $\epsilon'$  and (b) the  $\epsilon''$  of the PAN cloth carbonized in nitrogen at 600–800°C. [Color figure can be viewed in the online issue, which is available at [wileyonlinelibrary.com](http://wileyonlinelibrary.com).]

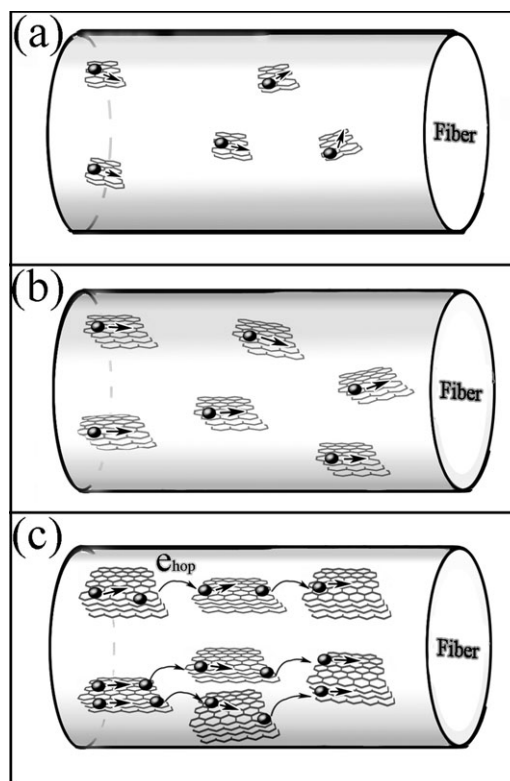


**Figure 6.** (a)–(c) Illustration showing the development of carbon sheets in ICPC.

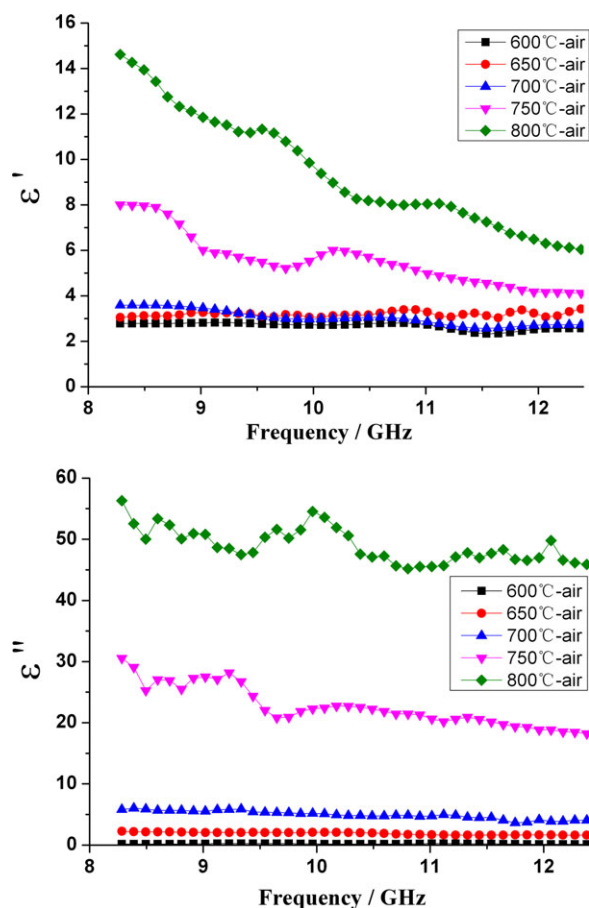


**Figure 7.** (a) The  $\epsilon'$  and (b) the  $\epsilon''$  of the PAN cloth carbonized in air at 600–800°C. [Color figure can be viewed in the online issue, which is available at [wileyonlinelibrary.com](http://wileyonlinelibrary.com).]

that in nitrogen at same carbonization temperature, which may be ascribed to the oxygen attack as discussed earlier. It can be observed from the conductivity results in Table II that the electrical conductivities of the fibers carbonized in air are about one magnitude lower than those carbonized in nitrogen at 650 to 750°C. Also, considering the results of XRD and Raman, the carbonization reaction of PNA may be restricted due to the attack of oxygen. This attack may not only lead to the visible deep pits on the surface [Figure 3(a)] but also break down the

**Table II.** Electric Conductivity of Carbon Fibers

Sample code	Electric conductivity of individual fiber $\sigma$ (S/m)
650°C-air	0.10–15
700°C-air	3–6
750°C-air	11–14
800°C-air	126–150
650°C-N <sub>2</sub>	2–4
700°C-N <sub>2</sub>	106–125
750°C-N <sub>2</sub>	153–176
800°C-N <sub>2</sub>	251–293

**Table III.** Reflection Loss Data of PCPC with Optimal Thickness

Sample code	Optimal thickness (mm)	RL in the 8–12 GHz (dB)	RL peak (dB)
600°C-air	5.2	<−1	<−2
650°C-air	4.0	<−10	−52
700°C-air	3.6	<−8	−11
750°C-air	2.4	<−3	−4
800°C-air	1.6	<−2	−3
600°C-N <sub>2</sub>	4.4	<−1	<−1
650°C-N <sub>2</sub>	2.8	<−6	−8
700°C-N <sub>2</sub>	2.4	<−2	−3
750°C-N <sub>2</sub>	1.2	<−2	−3
800°C-N <sub>2</sub>	0.8	<−1	−2

ladder chains structure and restrict the crosslink of these ladder chains to form carbon sheets. Moreover, the formed carbon sheets on the fiber surface also might be destroyed by the reaction with oxygen.

### Microwave Absorption

The calculated optimal reflection loss of ICPC as a single-layer absorber on the metal plane is summarized in Table III. The reflection loss below −10 dB (over 90% microwave absorption) in X band with minimum value of −52 dB can be obtained for the sample 650°C-air with the thickness of 4 mm. Conversely, the reflection loss of ICPC carbonized in air is evidently lower than that carbonized in nitrogen at the same temperature. Compared with the routine methods of carbonization in protective nitrogen, carbonization in low-pressure air has more advantages for fabricate microwave-absorbing materials. However, it must be noted that the carbonization must be carried out with strictly controlled air pressure, otherwise the PAN cloth is possible to be burnt out at high temperature.

Carbonization temperature also has significant influence on reflection loss as shown in Figure 8. The reflection loss is nearly

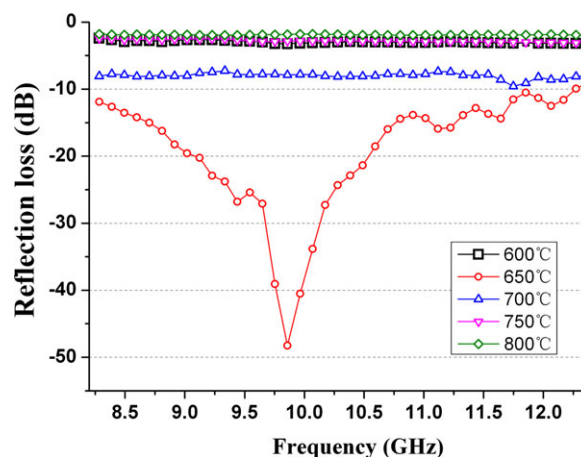


**Figure 8.** Calculated reflection loss of the samples carbonized in air at different temperature for 2 h (thickness = 4 mm). [Color figure can be viewed in the online issue, which is available at [wileyonlinelibrary.com](http://wileyonlinelibrary.com).]

0 dB for the cloth carbonized at 600°C, whereas it sharply drops below -10 dB in whole X band when the carbonization temperature increases to 650°C. The weak absorption can be ascribed to the small dielectric loss of the cloths carbonized at 600°C as shown in Figure 7. As the carbonization temperatures are higher than 650°C, the reflection loss sharply increases with the rising temperature. The increase of impedance mismatch between the composites and free space is responsible for this phenomenon because of the excessively large complex of these cloths as shown in Figure 7. It can be concluded that the optimal carbonization is 650°C in this research.

## CONCLUSIONS

The dielectric properties of the ICPC cloth are studied in X-band. Both carbonization temperature and atmosphere have great influence on the dielectric properties of ICPC. Generally, the complex permittivity of ICPC constantly increases with the increasing heating temperature due to the growth of carbon sheets. Conversely, the ICPC carbonized in the air exhibit lower complex permittivity than those carbonized in nitrogen because the attack of oxygen will restrict the growth of the carbon sheets in ICPC. The reflection loss below -10 dB with minimum value of -52 dB can be obtained for sample carbonized at 650°C in air. ICPC can be easily pasted on the objects while adding only a small amount of weight to the system, so we believe that the ICPC shall have great potential in many applications.

## ACKNOWLEDGMENT

This work was financially supported by the fund of the National Nature Science Foundation of China (No. 51072165) and the NPU Foundation for Fundamental Research (No.NPU-FFR-JC20110213).

## REFERENCES

- Zhao, D.-L.; Zhang, J.-M.; Li, X.; Shen, Z.-M. *J. Alloys Compd.* **2010**, *505*, 712.
- Liu, X.; Zhang, Z.; Wu, Y. *Compos. Part B-Eng.* **2011**, *42*, 326.
- Al-Ghamdi, A. A.; Al-Hartomy, O. A.; Al-Solamy, F.; Al-Ghamdi, A. A., El-Tantawy, F. *J. Appl. Polym. Sci.* **2013**, *127*, 2227.
- Raza, M. A.; Westwood, A. V. K.; Stirling, C.; Hondow, N. *Compos. Part A: Appl. Sci. Manuf.* **2011**, *42*, 1335.
- Micheli, D.; Apollo, C.; Pastore, R.; Marchetti, M. *Compos. Sci. Technol.* **2010**, *70*, 400.
- Meng, X.; Wan, Y.; Li, Q.; Wang, J.; Luo, H. *Appl. Surf. Sci.* **2011**, *257*, 10808.
- Liu, Y.; Zhang, Z.; Xiao, S.; Qiang, C.; Tian, L.; Xu, J. *Appl. Surf. Sci.* **2011**, *257*, 7678.
- Rahaman, M. S. A.; Ismail, A. E.; Mustafa, A. *Polym. Degrad. Stab.* **2007**, *92*, 1421.
- Gillespie, D. J.; Ehrlich, A. C. *J. Non-Cryst. Solids* **1992**, *144*, 231.
- Xie, W.; Cheng, H.; Chu, Z.; Chen, Z.; Long, C. *Ceram. Int.* **2011**, *37*, 1947.
- Tse-Hao, K.; Tzy-Chin, D.; Jeng-An, P.; Ming-Fong, L. *Carbon* **1993**, *31*, 765.
- Ko, T.-H.; Li, C.-H.; Hu, C.-H. *J. Mater. Res.* **1995**, *10*, 1529.
- Chieu, T. C.; Dresselhaus, M. S.; Endo, M. *Phys. Rev. B* **1982**, *26*, 5867.
- Tuinstra, F.; Koenig, J. *J. Chem. Phys.* **1970**, *53*, 1126.
- Sun, J. F.; Wu, G. X.; Wang, Q. R. *J. Appl. Polym. Sci.* **2005**, *97*, 2155.
- Zickler, G. A.; Smarsly, B.; Gierlinger, N.; Peterlik, H.; Paris, O. *Carbon* **2006**, *44*, 3239.
- Ferrari, A. C.; Robertson, J. *Phys. Rev. B* **2000**, *61*, 14095.
- Bashir, Z. *Carbon* **1991**, *29*, 1081.
- Breuer, O.; Sundararaj, U. *Polym. Compos.* **2004**, *25*, 630.
- Zhang, B.; Li, J.; Sun, J.; Zhang, S.; Zhai, H.; Du, Z. *J. Eur. Ceram. Soc.* **2002**, *22*, 93.
- Yang, Y. L.; Gupta, M. C.; Dudley, K. L.; Lawrence, R. W. *J. Nanosci. Nanotechnol.* **2005**, *5*, 927.